Materials Letters 231 (2018) 225–228

Contents lists available at ScienceDirect

Materials Letters

journal homepage: www.elsevier.com/locate/mlblue

Heterostructured HfO_2/TiO_2 spherical nanoparticles for visible photocatalytic water remediation

Devika Laishram, Kiran P. Shejale, Ritu Gupta, Rakesh K. Sharma *

Department of Chemistry, Indian Institute of Technology Jodhpur, NH-65, Nagaur Road, Karwar, Jodhpur, Rajasthan 342037, India

ARTICLE INFO

Article history:
Received 9 May 2018
Received in revised form 7 August 2018
Accepted 10 August 2018
Available online 11 August 2018

Keywords:
HfO_2/TiO_2
Hydrogenation
Photocatalytic dye degradation

ABSTRACT

Photocatalytic activity of low band gap hydrogenated HfO_2 doped TiO_2 (H-HfO_2/TiO_2), HfO_2 doped TiO_2 (HfO_2/TiO_2) and TiO_2 (pristine) were investigated by photocatalytic degradation of five different industrial dyes. The current study envisages the effect of doping hydrogen and HfO_2 up on TiO_2 for photocatalytic degradation of different chemically structured dyes. Methylene Blue attains fast degradation efficiency of 90%, within 10 min of the reaction due to high photocatalytic adsorption and degradation over the rough TiO_2 surface. Effect of pH on dye degradation is observed, leading to disintegration and mineralization.

1. Introduction

Chemical substances used in the textile and dyeing industries are mostly non-biodegradable which, when left untreated cause severe pollution to the aquatic ecosystem affecting health and environment [1]. On an average, 200 L of water is used for dyeing 1 kg of textiles [2]. The waste dyes in the water are either toxic, carcinogenic or changes the characteristic of water leaving it unfit for use for all practical purposes [3]. Traditional systems of water treatment such as flocculation, ion exchange and adsorption of dyes remain ineffective, costly and transfer nondestructively the pollution from one phase to another [4–6]. Thus, degradation of organic impurities into its various constituents like CO_2, water vapour and other inorganic substances via proper utilization of sunlight is a highly effective, low-cost solution. Recently, effective utilization of semiconductor photocatalysts has been resurgent of activity in water remediation [7–11]. TiO_2 is a principal semiconductor nanomaterial of choice because of its wide abundance, non-toxicity, high photocatalytic performance and stability [12–14]. However, TiO_2 suffers from low photocatalytic efficiency due to its wide band gap of 3.2 eV resulting in improper utilization of solar spectrum absorbing only in the UV range [15]. Thus, modification is for enhancing properties by doping various metals and non-metals, tuning the shape, morphology and particle size [16]. Recently, black TiO_2 synthesis has successfully reduced the band gap, expanding the absorptivity to visible range and increasing photoactivity [15–17].

In this work, the TiO_2 nanomaterial with 1% HfO_2 doping having most favourable structural and optical properties (2.94 eV, Fig. S2) is synthesized and tested for photo-degradation study of five different dyes – methyl orange (MO), methyl blue (MB), cresol red (CR), thymol blue (TB) and solochrome black (SB).

2. Experimental details

2.1. Synthesis of HfO_2/TiO_2 spherical nanoparticles (SNP)

H-HfO_2/TiO_2 nano-spherical structures were synthesized by sol-gel and solvothermal process [18]. Briefly, 1% HfO_2 doped TiO_2 were prepared by a two-step sol-gel and hydrothermal process followed by annealing under reducing hydrogen atmosphere. The detailed procedure is given in SI.

2.2. Characterization

The crystallographic parameters were analyzed by X-ray diffractometer (Bruker D8 Advance Diffractometer). Elemental composition analysis was performed using XRF (X-Ray Fluorescence) analyzer. Morphological analysis was done using TEM (Transmission Electron Microscopy, FEI Tecnai-G2 T20) operated at 200 kV. HPLC analysis was performed using Waters 2489 (Fig. S6), BET measurements were performed using Quantachrome Autosorb iQ3.

2.3. Photocatalytic degradation

The dyes – MO, MB, CR, SB and TB were purchased from Acros, SRL, Sigma and Qualigens. Dye solutions in water (20 μM) were

---

* Corresponding author.
E-mail address: rks@iitj.ac.in (R.K. Sharma).

https://doi.org/10.1016/j.matlet.2018.08.053
0167-577X/

prepared and 400 mg/L of catalyst was dispersed in 15 mL of each of the dye solutions. The photocatalytic behavior was observed under 1 Sun simulated light (SS50AAA Solar Simulator, PET Photo Emission Tech.) for 50 min under mild stirring. The residual concentration of the dye was estimated by a colorimeter.

3. Results and discussion

3.1. Structural and Morphological characterization

The material showed lattice planes distinct to anatase phase of TiO_2 which is identified with JCPDS 021-1272 (Fig. 1a). No extra peaks were observed in the diffraction pattern of TiO_2 SNP and thus it can be concluded that the material synthesized is highly pure [19]. HfO_2/TiO_2 and H-HfO_2/TiO_2 showed broad hump at 28.3° and 31.62° ascertained to monoclinic HfO_2 [20]. The effect on strain and crystallite size upon doping HfO_2 and eventual hydrogenation are observed and tabulated in Fig. 1b and Table 1. The magnified (1 0 1) highest intense peak (Fig. 1b) showed 2 θ shift in the lower angle corresponding to ~0.04 and ~0.128 after doping HfO_2 and hydrogenation correspondingly. XRF plot in Fig. 1c indicates presence of Hf ($L_{\alpha1}$ and $L_{\beta1}$) and Ti ($K_{\alpha1}$ and $K_{\beta1}$) in the synthesized SNP.

Lattice expansion of 0.0738% was observed for H-HfO_2/TiO_2 due to incorporation of bigger size HfO_2 on the TiO_2 lattice [21]. Moreover, annealing under reducing hydrogen atmosphere creates defects in lattice contributing substantially to lattice expansion [17]. The XRF spectroscopy is a non-destructive analysis technique that gives quantitative and qualitative assessment of elements. The intense peak showed the presence of larger amount of Ti in the sample and Hf as smaller humps due to 1% doping in the prepared SNP.

The uniformly formed spherical morphology of the materials was confirmed using TEM (Fig. 2a–c) that showed TiO_2 SNP comprising of smaller grain like TiO_2 and HfO_2 particles. Fig. 2a–c (inset) revealed the gradual increase in size of the SNP upon doping, with H-HfO_2/TiO_2 being the largest. The average diameter follows the order – TiO_2 (~305 nm) < HfO_2/TiO_2 (~326 nm) < H-HfO_2/TiO_2 (~400 nm). Also, even distribution of pores was observed by the light and dark contrast in TEM images. The HR-TEM images (Fig. 2d–f) indicate lattice spacing corresponding to anatase phase of TiO_2 with average d-spacing value of 0.35 nm consistent to (1 0 1) as observed in the XRD pattern (Fig. 2a). The bright spots in SAED pattern (Fig. S1a–c) are fainted upon hydrogen treatment due to slight decrease in polycrystalline nature which is understandable.

3.2. Photocatalytic activity

Aqueous solution of various dyes – MB, CR, MO, TB and SB were photocatalytically degraded using the synthesized materials as catalyst for 50 min (Fig. 3a–c). Amongst all dyes, MB was best degraded by all the three catalysts within shortest duration observed for H-HfO_2/TiO_2 with 90% in 10 min. MB shows strong absorbance at 664 nm and 292 nm with shoulder peak at 614 nm and 245 nm (Fig. 3(d–f)). The adsorption of dye upon the catalyst surface depends on the electrostatic interaction between the dye and surface of the catalyst [22]. TiO_2 is amphoteric and reacts differently with pH, e.g. MB is cationic and adsorption is stronger with TiO_2 surface leading to higher degradation efficiency under basic conditions (Fig. 3d–f). Catalyst containing dye gets degraded when electron-hole pair generated by the light reacts with water molecules to yield active radicals. The oxidation of dyes lead to cleavage of bonds and breaking of aromatic rings with formation of smaller inorganic molecules in three steps–decolourization, degradation and mineralization. Enhanced degradation activity of H-HfO_2/TiO_2 with a band gap of 2.47 eV (Fig. S2) was observed due to better utilization of solar spectrum, reduced recombination and suitable tuning of band gap due to annealing under hydrogen and doping HfO_2. Hydrogen annealing leads to formation of defect and oxygen vacant sites creating superoxide and hydroxyl radicals useful for dye degradation [17,23]. Thus, H-HfO_2/TiO_2 showed the

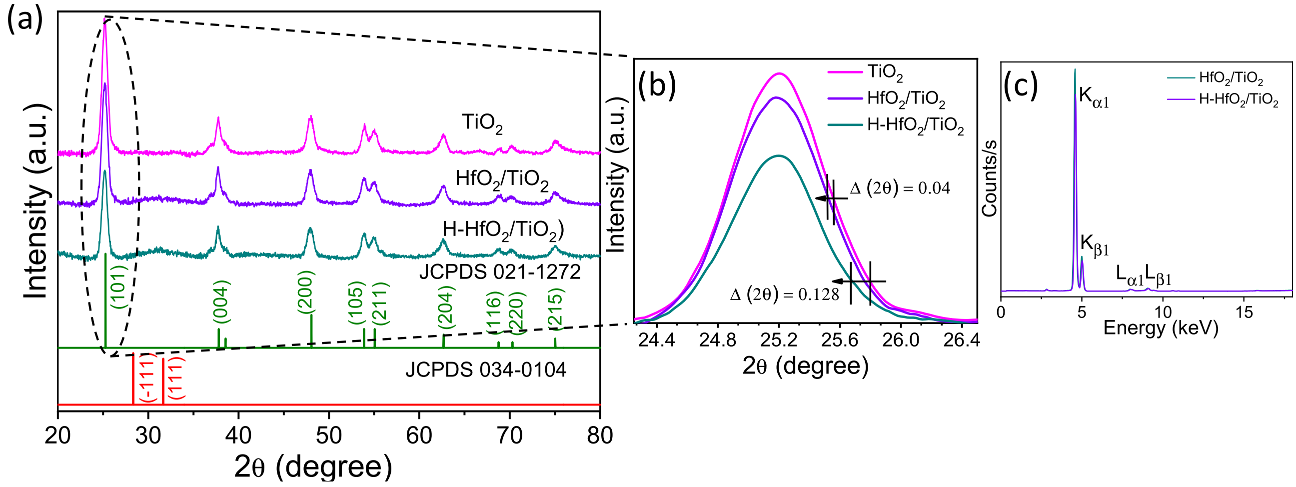

Fig. 1. (a) XRD of the material with JCPDS data (b) XRD of highest intense peak (1 0 1) denoting shift and intensity change. (c) XRF spectra of doped TiO_2.

Table 1
Cell parameters of the nanomaterials.

Sl. No.	Synthesized SNP	Crystallite Size (in nm)	Strain	Unit cell parameter calculated	
				a (nm)	c (nm)
1.	TiO_2	3.2018	0.5259 ± 0.2351	0.3789	0.8815
2.	HfO_2/TiO_2	3.0188	0.4137 ± 0.2530	0.3790	0.9710
3.	H- HfO_2/TiO_2	3.4863	0.5272 ± 0.2144	0.3792	0.9715

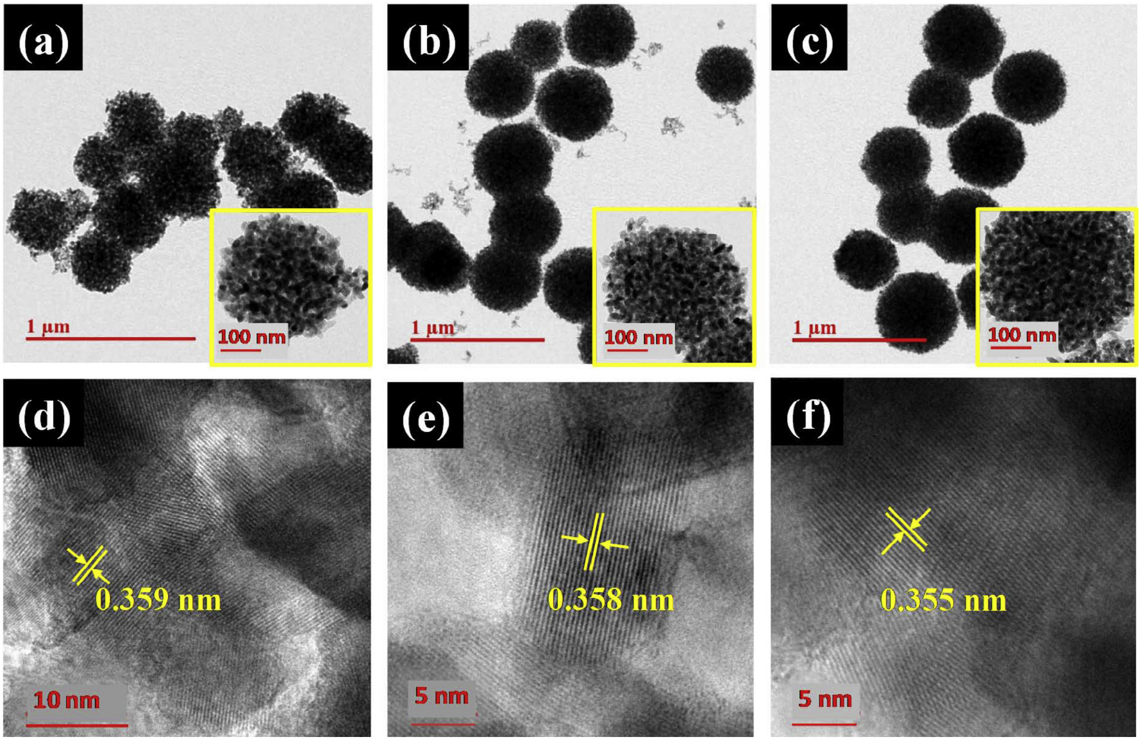

Fig. 2. TEM (a), (b), (c) and HR-TEM (d), (e), (f) images of synthesized TiO_2, HfO_2/TiO_2 and H-HfO_2/TiO_2 respectively. Inset of (a), (b) and (c) shows the corresponding spherical structure growing in size with doping.

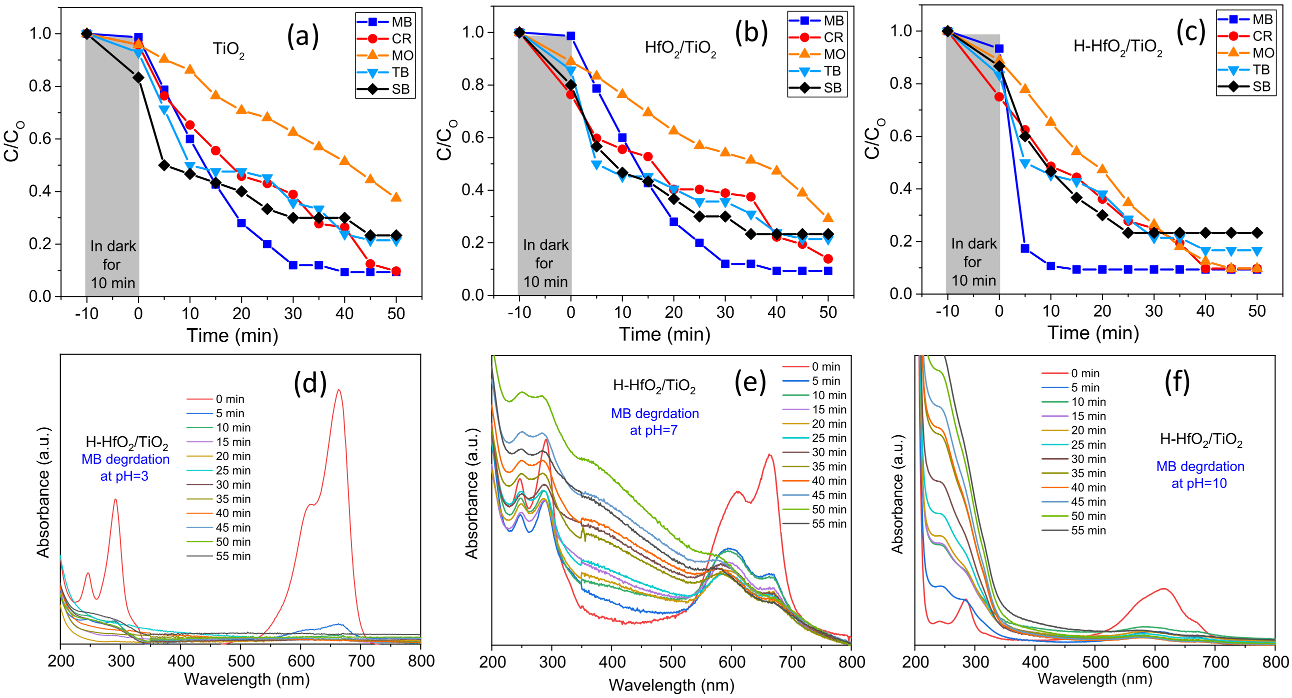

Fig. 3. (a–c) Degradation of five different dyes using TiO_2, HfO_2/TiO_2 and H-HfO_2/TiO_2 at pH ~7. (d-f) show the degradation of MB dye at different pH using H-HfO_2/TiO_2.

highest degradation rate at 0.216 min^{-1} among the three catalysts tested with MB dye (Table S1). Also, the % degradation efficiency was calculated and plotted (Fig. S4) for each of the five dyes degraded using all catalysts. Recyclability test was performed for five cycles for MB with H-HfO_2/TiO_2, revealed high stability of catalyst (Fig. S5). Obliteration of dye to smaller molecules due to photocatalytic degradation can be realized by the appearance of new peaks at lower retention time in the HPLC chromatogram (Fig. S6). Additionally, the improved degradation efficiency using H-HfO_2/TiO_2 is attributed to the HfO_2 doping leading to a highly mesoporous structure with larger surface area for exchange of mass between the dye and catalyst molecules as confirmed from the BET analysis (Fig. S3, Table S2) [24,25]. Moreover, doping induced defects and oxygen vacancies act as trapping sites decreasing the recombination rate. Thus, the compound effect of doping HfO_2 over TiO_2 and subsequent annealing under H_2 atmosphere can be a suitable means to synthesize an advanced form of SNP for using in accelerated photocatalytic dye degradation applications. The results are compared with literature reports and tabulated in Table S3.

4. Conclusion

High surface area nanospherical black TiO_2 doped with 1% HfO_2 are synthesized by sol-gel and hydrothermal method for degradation of five common textile dyes. The morphological characterizations using TEM analysis revealed that each nanosphere has an average size of ~500 nm consisting of 15–20 nm size granules of HfO_2 and TiO_2 nanoparticles. Such structural assembly greatly enhances the number of active sites, surface area for dye attachment and enhances the light scattering effect. Degradation study of the dyes revealed high activity over 90% within 10 min for MB under illumination at basic pH.

Acknowledgement

The authors would like to thank Indo-UK NERC Water Quality Project DST/TM/INDO-UK/2K17/52 for financial support and MRC, MNIT Jaipur, India, for TEM facility and CASE, IIT Jodhpur for characterization facility. Authors gratefully acknowledge Mr. Ganpat Choudhary and Mr. Shubham Pandey for XRD and BET analysis.

Appendix A. Supplementary data

Supplementary data associated with this article can be found, in the online version, at https://doi.org/10.1016/j.matlet.2018.08.053.

References

[1] M. Saquib, M.A. Tariq, M.M. Haque, M. Muneer, J. Environ. Manage. 88 (2008) 300–306.
[2] C. Parvathi, T. Maruthavanan, C. Prakash, The Indian Textile Journal November 2009.
[3] L.Y. Yang, S.Y. Dong, J.H. Sun, J.L. Feng, Q.H. Wu, S.P.J. Sun, J. Hazard. Mater. 179 (2010) 438–443.
[4] V. Meshko, L. Markovska, M. Mincheva, A.E. Rodrigues, Water Res. 35 (2001) 3357–3366.
[5] S. Raghu, C.A. Basha, J. Hazard. Mater. 149 (2007) 324–330.
[6] F. Harrelkas, A. Azizi, A. Yaacoubi, A. Benhammou, Desalination 235 (2009) 330–339.
[7] D. Ljubas, G. Smoljanic, H. Juretic, J. Environ. Manage. 161 (2015) 83–91.
[8] J. Tian, Y.H. Leng, H.Z. Cui, H. Liu, J. Hazard. Mater. 299 (2015) 165–173.
[9] X. Hu, H. Zhao, J. Tian, J. Gao, Y. Li, H. Cu, Sol. Energy Mater. Sol. Cells. 172 (2017) 108–116.
[10] Y. Ide, N. Inami, H. Hattori, K. Saito, M. Sohmiya, N. Tsunoji, et al., Angew. Chem. Int. Ed. 55 (2016) 3600–3605.
[11] J.T. Park, D.J. Kim, D.H. Kim, J.H. Kim, Mater. Lett. 202 (2017) 66–69.
[12] H. Hadjltaief, M.B. Zina, M.E. Galvez, P.D. Costa, J. Photochem. Photobiol., A 315 (2016) 25–33.
[13] Q. Guo, C. Zhou, Z. Ma, Z. Ren, H. Fan, X. Yang, Chem. Soc. Rev. 45 (2016) 3701–3730.
[14] C.C. Raj, R. Prasanth, J. Power Sour. 317 (2016) 120–132.
[15] T. Leshuk, R. Parviz, P. Everett, H. Krishnakumar, R.A. Varin, F. Gu, ACS Appl. Mater. Interfaces 5 (2013) 1892–1895.
[16] Y. Sang, H. Liu, A. Umar, ChemCatChem 7 (2015) 559–573.
[17] X. Chen, L. Liu, P.Y. Yu, S.S. Mao, Science 331 (2011) 746–750.
[18] D. Laishram, K.P. Shejale, R.K. Sharma, R. Gupta, RSC Adv. 6 (2016) 78768–78773.
[19] T. Su, Y. Yang, Y. Na, R. Fan, L. Li, L. Wei, et al., ACS Appl. Mater. Interfaces 7 (2015) 3754–3763.
[20] Y. Wan, X. Zhou, RSC Adv. 7 (2017) 7763–7773.
[21] A. Latini, C. Cavallo, F.K. Aldibaja, D. Gozzi, J. Phys. Chem. C 117 (2013) 25276–25289.
[22] N. Wang, F. Tan, Yu Zhao, C.C. Tsoi, X. Fan, W. Yu, X. Zhang, Sci. Rep. 6 (2016) 28928.
[23] K. Zhang, J.H. Park, J. Phys. Chem. Lett. 8 (2017) 199–207.
[24] G. Panomsuwan, A. Watthanaphanit, T. Ishizakiae, N. Saito, Phys. Chem. Chem. Phys. 17 (2015) 13794–13799.
[25] B. Sambandam, A. Surenjan, L. Philip, T. Pradeep, ACS Sustainable Chem. Eng. 3 (2015) 1321–1329.